



# Carbon Monoxide Attenuates High Salt-Induced Hypertension While Reducing Pro-inflammatory Cytokines and Oxidative Stress in the Paraventricular Nucleus

Dong-Dong Zhang<sup>1,3</sup> · Yan-Feng Liang<sup>1,4</sup> · Jie Qi<sup>1</sup> · Kai B. Kang<sup>5</sup> · Xiao-Jing Yu<sup>1</sup> · Hong-Li Gao<sup>1</sup> · Kai-Li Liu<sup>1</sup> · Yan-Mei Chen<sup>1</sup> · Xiao-Lian Shi<sup>6</sup> · Guo-Rui Xin<sup>1</sup> · Li-Yan Fu<sup>1</sup> · Yu-Ming Kang<sup>1</sup> · Wei Cui<sup>2</sup>

Published online: 29 April 2019

© Springer Science+Business Media, LLC, part of Springer Nature 2019

## Abstract

Carbon monoxide (CO) presents anti-inflammatory and antioxidant activities as a new gaseous neuromessenger produced by heme oxygenase-1 (HO-1) in the body. High salt-induced hypertension is relevant to the levels of pro-inflammatory cytokines (PICs) and oxidative stress in the hypothalamic paraventricular nucleus (PVN). We explored whether CO in PVN can attenuate high salt-induced hypertension by regulating PICs or oxidative stress. Male Dahl Salt-Sensitive rats were fed high-salt (8% NaCl) or normal-salt (0.3% NaCl) diet for 4 weeks. CORM-2, ZnPP IX, or vehicle was microinjected into bilateral PVN for 6 weeks. High-salt diet increased the levels of MAP, plasma norepinephrine (NE), reactive oxygen species (ROS), and the expressions of COX2, IL-1 $\beta$ , IL-6, NOX2, and NOX4 significantly in PVN ( $p < 0.05$ ), but decreased the expressions of HO-1 and Cu/Zn-SOD in PVN ( $p < 0.05$ ). Salt increased sympathetic activity as measured by circulating norepinephrine, and increased the ratio of basal RSNA to max RSNA, in part by decreasing max RSNA. PVN microinjection of CORM-2 decreased the levels of MAP, NE, RSNA, ROS and the expressions of COX2, IL-1 $\beta$ , IL-6, NOX2, NOX4 significantly in PVN of hypertensive rat ( $p < 0.05$ ), but increased the expressions of HO-1 and Cu/Zn-SOD significantly ( $p < 0.05$ ), which were all opposite to the effects of ZnPP IX microinjected in PVN ( $p < 0.05$ ). We concluded that exogenous or endogenous CO attenuates high salt-induced hypertension by regulating PICs and oxidative stress in PVN.

**Keywords** Carbon monoxide · High salt-induced hypertension · Hypothalamic paraventricular nucleus (PVN) · Pro-inflammatory cytokines (PICs) · Oxidative stress

---

Handling Editor: Rajiv Janardhanan.

---

**Electronic supplementary material** The online version of this article (<https://doi.org/10.1007/s12012-019-09517-w>) contains supplementary material, which is available to authorized users.

---

Dong-Dong Zhang and Yan-Feng Liang have contributed equally to this work.

- 
- ✉ Jie Qi  
jie-qi@xjtu.edu.cn
  - ✉ Yu-Ming Kang  
ykang@mail.xjtu.edu.cn
  - ✉ Wei Cui  
doctorweimei.cui@126.com

Extended author information available on the last page of the article

## Introduction

As a complex genetic disease, hypertension was affected by many environmental factors including high-salt diet [1, 2]. Although the molecular mechanisms of high salt-induced hypertension were unclear in the central nervous system (CNS), a growing body of evidence suggests that it is associated with inflammation and oxidative stress in the hypothalamic paraventricular nucleus (PVN) [3, 4]. In the brain, the PVN is reciprocally connected to other areas of the CNS, which is involved in modulating the mean arterial pressure (MAP) [5, 6] and sympathetic nerve activity [7] as a principal cardiovascular center.

Carbon monoxide (CO), a byproduct of heme oxygenase (HO), is now being considered a new gaseous neural messenger in the brain [8], which is previously thought to be a toxic gas and biological waste product. The predominant source of CO in animals is heme degradation,

which is catalyzed by the rate-limiting enzyme HO. Three forms of HO have been identified including HO-1, HO-2, and HO-3. As the only inducible enzyme among the three, HO-1 showed high expression in some tissues when it was induced by heme or numerous oxidative stressors [9]. Previous studies have reported that HO-1 has been found in specific groups of CNS neurons, particularly within the paraventricular nucleus (PVN), supraoptic nucleus (SON), ventromedial nuclei, and preoptic nuclei [10, 11]. There has been a speculation that endogenous CO of peripheral circulation decreased blood pressure (BP), which is mediated by autonomic nervous function [9, 12]. But the effects and mechanisms of CO on sympathetic nerve activity (SNA) and BP in the PVN are not very clear.

It has been considered that the pro-inflammatory cytokines (PICs), such as interleukin-1beta (IL-1 $\beta$ ) and interleukin-6 (IL-6), contribute to the hypertensive effects [13]. And oxidative stress has been considered as critical factors in hypertensive responses [14–16]. Furthermore, our previous study has shown that the levels of PICs and reactive oxygen species (ROS), the key mediators of oxidative stress, within the PVN were also responsible for the hypertensive responses [6, 17, 18]. CO has been identified to present antioxidant, anti-inflammatory, and anti-tumor properties [19–26]. However, HO-1 is a widely distributed enzyme that catabolizes heme to bilirubin, CO, and free iron. And it has been reported that biliverdin was an antioxidant and may potentially decrease BP [27, 28]. Thus, Carbon monoxide-releasing molecule-2 (CORM-2) was used as the donor of exogenous CO released from tricarbonyldichlororuthenium (II) dimer to confirm the effects of CO in this study. Zinc protoporphyrin IX (ZnPP IX) inhibits heme oxygenase and then permits the assessment of the endogenous CO synthesis. We explored whether exogenous and endogenous CO in the PVN regulates the levels of PICs or oxidative stress in PVN during the pathogenesis of hypertension to further elaborate the molecular mechanisms of high salt-induced hypertension.

## Materials and Methods

### Animals

Experiments were carried out on healthy adult male Dahl Salt-Sensitive rats (Charles River Laboratories International, Inc., Wilmington, MA, USA) weighing from 250 to 275 g. The rats were kept in temperature ( $23 \pm 2$  °C) and light-controlled (12 h–12 h light–dark cycle) with standard rat chow and tap water ad libitum. All experimental procedures were approved by the Institutional Animal Care and Use Committees of Xi'an Jiaotong University. The procedures were

complied with the Guide for the Care and Use of Laboratory Animals published by the US National Institutes of Health (NIH Publication No. 85-23, revised 1996).

### General Experimental Protocol

The male Dahl Salt-Sensitive rats were randomized to one of the following six groups: NS + PVN vehicle group, NS + PVN CORM-2 group, NS + PVN Zinc protoporphyrin IX (ZnPP IX) group, HS + PVN vehicle group, HS + PVN CORM-2 group, and HS + PVN ZnPP IX group. The rats in NS groups were fed normal-salt diet (NS, 0.3% NaCl), while the rats in HS groups were fed high-salt diet (HS, 8% NaCl). CORM-2 (2 nmol/h; dissolved in 0.5% dimethyl sulfoxide in artificial cerebrospinal fluid (aCSF); Sigma-Aldrich, USA), the CO donor, was microinjected in the bilateral PVN of rats at the end of the 4th week after anesthetized with a ketamine (80 mg/kg) and xylazine (10 mg/kg) mixture via intraperitoneal injection (ip) for 6 weeks by the cannula connected with the osmotic minipumps (ALZET, model 2006) for chronic infusion, while ZnPP IX (2 nmol/h; Sigma-Aldrich, USA), an inhibitor of HO-1, was microinjected in PVN of rats according to the same principles. The dosages were based on the other two effective studies [29, 30]. At the end of 10 weeks, the blood and the brain tissue of the rats were collected for immunofluorescence, immunohistochemical analysis, ELISA, and molecular studies after anesthesia and euthanasia. The tissues were collected from both sides of the PVN of individual rat and stored at  $-80$  °C until assayed.

### Bilateral PVN Microinjection

The method for implantation of bilateral PVN cannulae has been described previously [31, 32]. The head of the rat was placed into a stereotaxic apparatus after the rat was anesthetized with a ketamine (80 mg/kg) and xylazine (10 mg/kg) mixture (ip). The skull was opened, and a stainless steel cannula connected with an osmotic minipump was microinjected into the PVN according to stereotaxic coordinates, which was approximately 1.8 mm posterior to the bregma, 0.4 mm lateral to the central line, and 7.9 mm ventral to the zero level. The osmotic minipumps were filled with CORM-2, ZnPP IX, or vehicle and implanted subcutaneously in the back of the neck, which would maintain the infusion to the PVN for 6 weeks continuously. The cannula was fixed to the cranium using dental acrylic. After the surgery was finished, all rats received buprenorphine (0.01 mg/kg, sc) immediately and 12 h postoperatively. Only animals with verifiable bilateral PVN injection sites were used in the final analysis. The success rate of bilateral PVN microinjection was 75%.

## Mean Arterial Pressure (MAP) Measurement

Mean arterial pressure measurement (MAP) of the rats has been described previously [4]. MAP was collected for 30 min between 8 and 11 a.m. and averaged. MAP of the rat was determined noninvasively weekly by a tail-cuff occlusion method via an automatic sphygmomanometer. Blood pressure values were averaged from six consecutive cycles per week obtained from each rat. The tail artery systolic blood pressure was measured daily for at least 7 days so that the stress-induced blood pressure fluctuations were minimized. Unanesthetized rats were placed in a holding device mounted on a thermostatically controlled warming plate (38 °C), which achieved the steady pulse. At the end of 10 weeks the femoral artery cannula was connected to a pressure transducer (MLT0380, ADInstruments, Australia) and flushed with 0.1 ml heparinized saline (50 U/ml). The cannula was catheterized in the femoral artery to measure the BP after the rat was anesthetized with a ketamine (80 mg/kg) and xylazine (10 mg/kg) mixture (ip).

## Renal Sympathetic Nerve Activity (RSNA) Recordings

The general methods of recording and analyzing renal sympathetic nerve activity (RSNA) have been described previously [33]. The left renal nerve of rat was isolated using a glass microelectrode under an inversion microscope after anesthesia and laparotomy. The renal nerve was cut distally to eliminate its afferent activity and hung by a platinum electrode that is connected with the recording system. The nerve was then covered by paraffin oil tampons to isolate electrical disturbance and moisturize the nerve. The sodium nitroprusside (SNP) (KELUN, Hunan, China) was administered as a 10- $\mu$ g intravenous bolus via the common jugular vein to detect maximum RSNA. At the end of the experiment, the background noise was defined after section of the central end of the nerve RSNA was subtracted from actual RSNA. The result of RSNA was subsequently expressed as percent of maximum, which was used in the experimental analysis. The data recording and analysis of RSNA were detected by BL-420 Biological Function Experiment System (BL-420E+, Chengdu Techman, China).

## ELISA Analysis

The circulating plasma levels of norepinephrine (NE) are detected by commercially available rat ELISA kits (Invitrogen, USA) as described previously [34]. Plasma samples were collected and stored at  $-80$  °C. The standard and

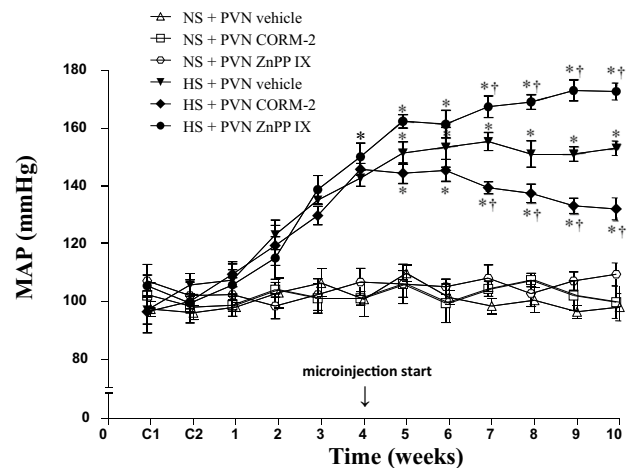


**Fig. 1** Effects of PVN infusion of CORM-2, ZnPP IX, or vehicle on mean arterial pressure (MAP) in high-salt diet (HS, 8% NaCl) or a normal-salt diet (NS, 0.3% NaCl) rats. MAP was increased significantly after 4 weeks in HS rats compared to NS rats ( $p < 0.05$ , each group  $n = 7$ ). MAP was decreased significantly in the HS+PVN CORM-2 group, but increased in the HS+PVN ZnPP IX group, as compared to the HS+PVN vehicle group ( $p < 0.05$ , each group  $n = 7$ ). Values are expressed as mean  $\pm$  SEM. \* $p < 0.05$  versus control (NS groups); † $p < 0.05$  HS+PVN CORM-2 or ZnPP IX versus HS+PVN vehicle

samples were transferred to a 96-well assay microplate coated with NE-specific antibody according to the manufacturer's instructions. And then the microplate was incubated at 37 °C and washed. Then horseradish peroxidase (HRP)-conjugated reagent was added. The microplate was incubated and washed again. And the chromogenic solution, stop solution was added sequentially in the microplate to stop the reaction. The optical density (OD) at 450 nm was then read using an ELISA microplate reader (MK3, Thermo Scientific, USA).

## Immunofluorescence and Immunohistochemistry Analysis

The method of immunofluorescence and immunohistochemistry has been described previously [18]. Rats received a thoracotomy under general anesthesia. A cannula was inserted into the left ventricle of the rat that connected to a transfusion device added sequentially 0.1 M phosphate-buffered solution (PBS) and 4% paraformaldehyde at pH 7.4 under anesthesia. The brains were removed and immersed immediately in 4% paraformaldehyde for 1 h and then in 30% sucrose for 2 days. Remaining samples were used for Cryostat sections (10  $\mu$ m) which were put on slides, and stored at  $-80$  °C for future use for immunofluorescence. For each animal, labeled neurons within the

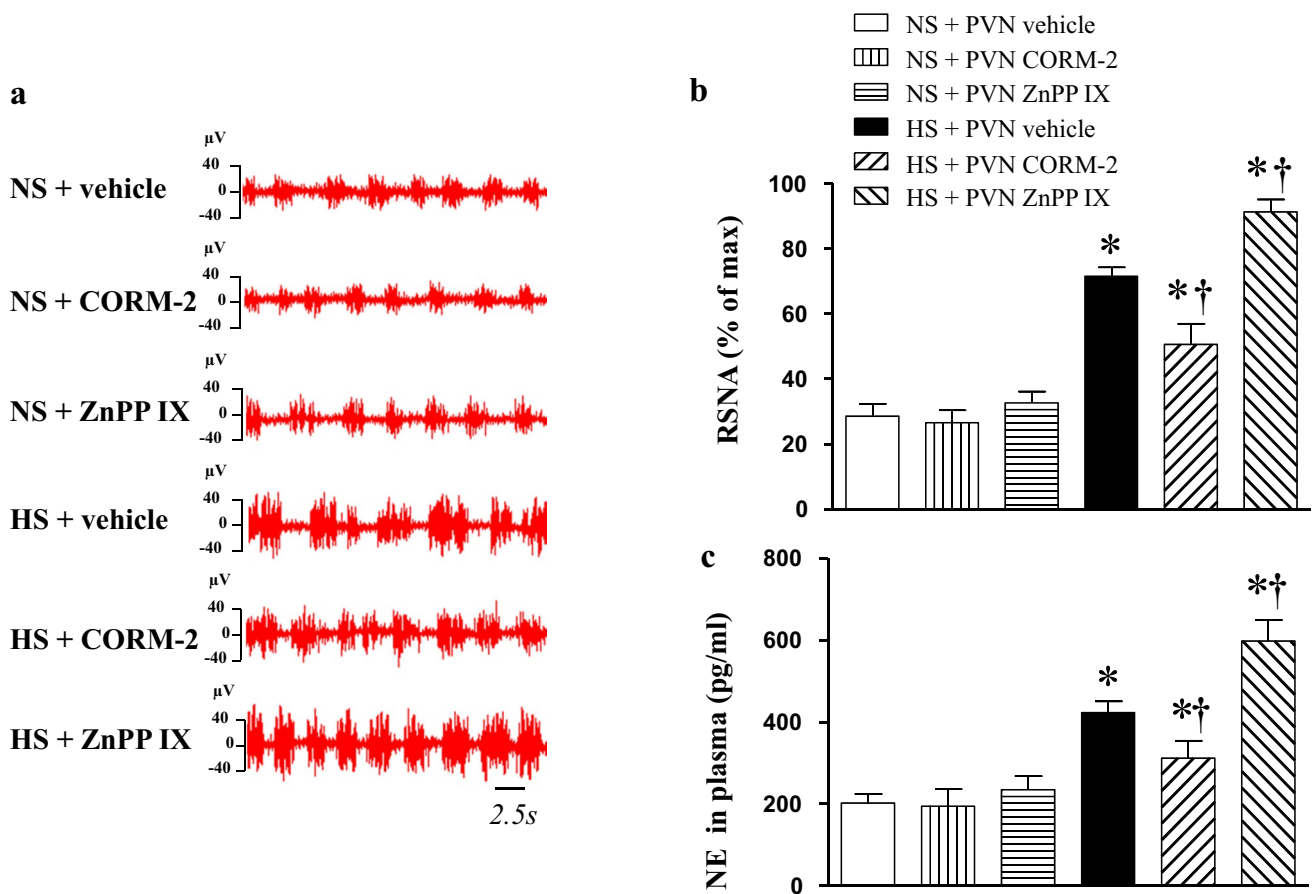


**Fig. 2** Effects of PVN infusion of CORM-2, ZnPP IX, or vehicle on the RSNA and plasma NE. **a** The results of renal sympathetic nervous activity (RSNA) were detected by BL-420E+. **b** The RSNA in high-salt diet rats were higher than in normal-salt diet rats, but decreased significantly in the HS + CORM-2 group and increased significantly in the HS + ZnPP IX group ( $p < 0.05$ , each group  $n = 7$ ). **c** The lev-

els of plasma NE were higher in high-salt diet rats than in normal-salt diet rats, but decreased significantly in the HS + CORM-2 group and increased significantly in the HS + ZnPP IX group ( $p < 0.05$ , each group  $n = 7$ ). \* $p < 0.05$  versus control (NS groups); † $p < 0.05$  HS + PVN CORM-2 or ZnPP IX versus HS + PVN vehicle

**Table 1** Effects of PVN infusion of CORM-2, ZnPP IX, or vehicle on the max RSNA response to SNP

Group	NS + PVN vehicle	NS + PVN CORM-2	NS + PVN ZnPP IX	HS + PVN vehicle	HS + PVN CORM-2	HS + PVN ZnPP IX
N	7	7	7	7	7	7
Spikes/s	278 ± 10	275 ± 6	286 ± 13	227 ± 7*	243 ± 8*	236 ± 8*

Values are expressed as mean ± SEM

\* $p < 0.05$  versus control (NS groups)

borders of PVN bilaterally were counted manually in two representative transverse sections at about  $-1.80$  mm from bregma, and an average value was reported. The primary antibody of heme oxygenase-1 (HO-1, bs-0827R-FITC) was from Bioss antibodies. The primary antibody of COX2 (No. ab15191) was from Abcam. The other primary antibodies were all from Santa Cruz Biotechnology including IL-1 $\beta$  (sc-1251), IL-6 (sc-1265), NOX2 (sc-5827), NOX4

(sc-21860), Cu/Zn-SOD (sc-11407). Reactive oxygen species (ROS) in the PVN was detected by fluorescent-labeled dihydroethidium (DHE; molecular probes) staining. Immunohistochemistry stained sections were photographed with a conventional light microscopy (DP70, Olympus, Tokyo, Japan). Immunofluorescent staining was visualized with a confocal laser-scanning microscope (Zeiss LSM 710, Carl Zeiss, Inc).

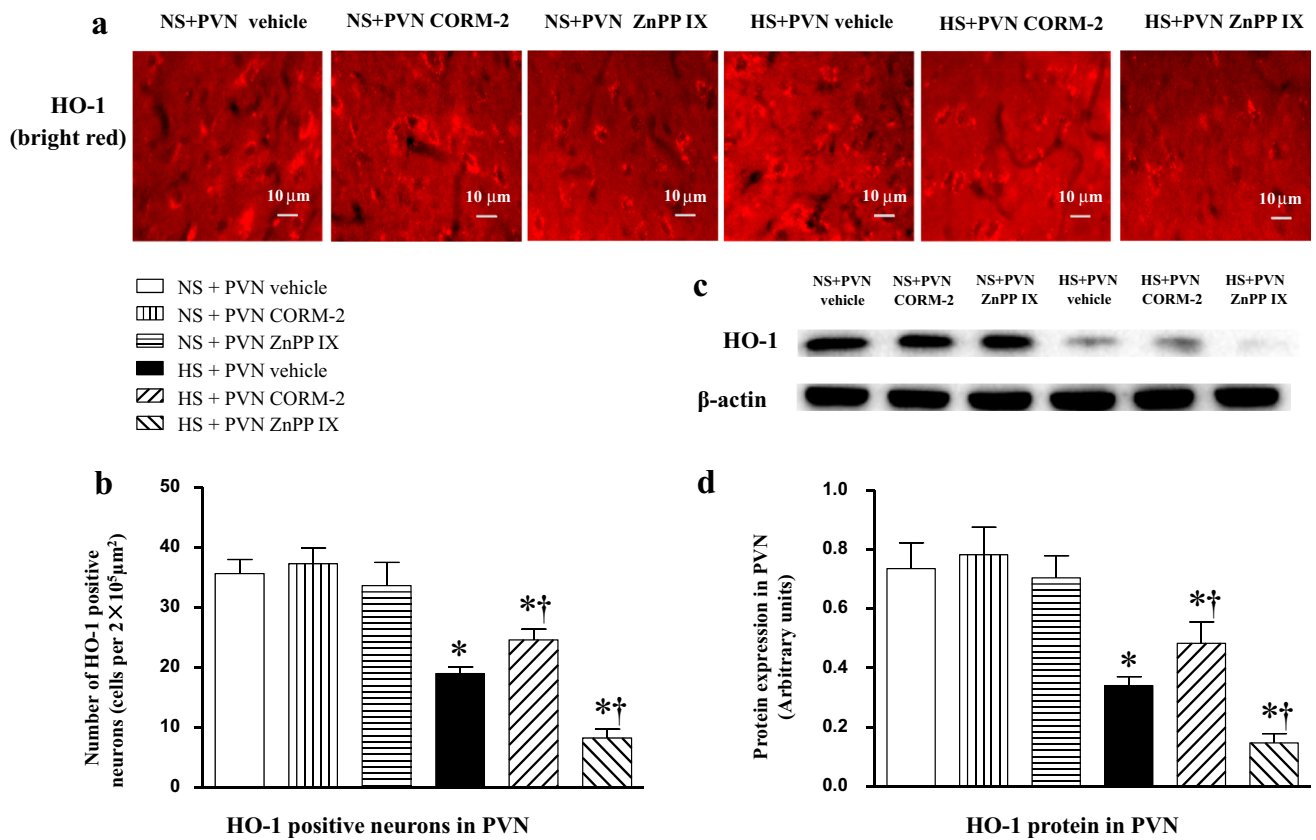


**Fig. 3** Effects of PVN infusion of CORM-2, ZnPP IX, or vehicle on the expressions of HO-1 in PVN. The expressions of PVN HO-1 in high-salt diet rats were lower than in normal-salt diet rats, but increased significantly in the HS+CORM-2 group and decreased significantly in the HS+ZnPP IX group ( $p < 0.05$ , each group  $n = 7$ ). **a** Representative immunofluorescence staining of HO-1. **b** Densito-

metric analysis of immunofluorescent intensity of HO-1 in the PVN. **c** A representative immunoblot of HO-1 in the PVN. **d** Densitometric analysis of protein expression of HO-1 in the PVN. Values are expressed as mean  $\pm$  SEM. \* $p < 0.05$  versus control (NS groups); † $p < 0.05$  HS + PVN CORM-2 or ZnPP IX versus HS + PVN vehicle

### Western Blot Analysis

The rats were euthanized. The PVN tissues were quickly collected and submerged in liquid nitrogen and followed by storing at  $-80^\circ\text{C}$ . The frozen brain of rat was cut with a cryostat until the third ventricle(3 V) was exposed. The brain was sectioned serially in 300 μm increments from the bregma to lambda. The sections were transferred to glass slides and placed on a cold stage maintained at  $-10^\circ\text{C}$ . According to the atlas of “the rat brain in stereotaxic coordinates,” the PVN sites were easy to detect and to be collected and submerged in liquid nitrogen, followed by storing at  $-80^\circ\text{C}$ . Proteins extracted from PVN tissue were used for western blot analysis after the concentrations were modified by BCA protein assay. As described previously [4, 34], protein samples were separated by SDS-PAGE and transferred to a polyvinylidene fluoride (PVDF) membrane. Membranes were blocked with TBST buffer (TBS plus 0.1% Tween-20) containing 5.0% dried skim milk for 2 h followed by washing

with TBST at room temperature. The primary antibodies, referring to the antibodies in the IHC section, were then added on the membranes and incubated overnight at  $4^\circ\text{C}$ . The appropriate horseradish peroxidase-conjugated secondary antibodies were added after washing. Bands were visualized by enhanced chemiluminescence using ChemiDoc XRS System (Bio-rad, USA). Band densities were analyzed using ImageJ Image Analysis Software (NIH). Protein levels were presented after normalization to β-actin (Santa Cruz Biotechnology, Santa Cruz, CA).

### Statistical Analysis

All data were expressed as mean  $\pm$  SEM. MAP data were analyzed by repeated measures ANOVA. The significance of differences between mean values was analyzed by ANOVA followed by a post hoc Tukey’s test. A probability value of  $p < 0.05$  was considered as statistically significant.

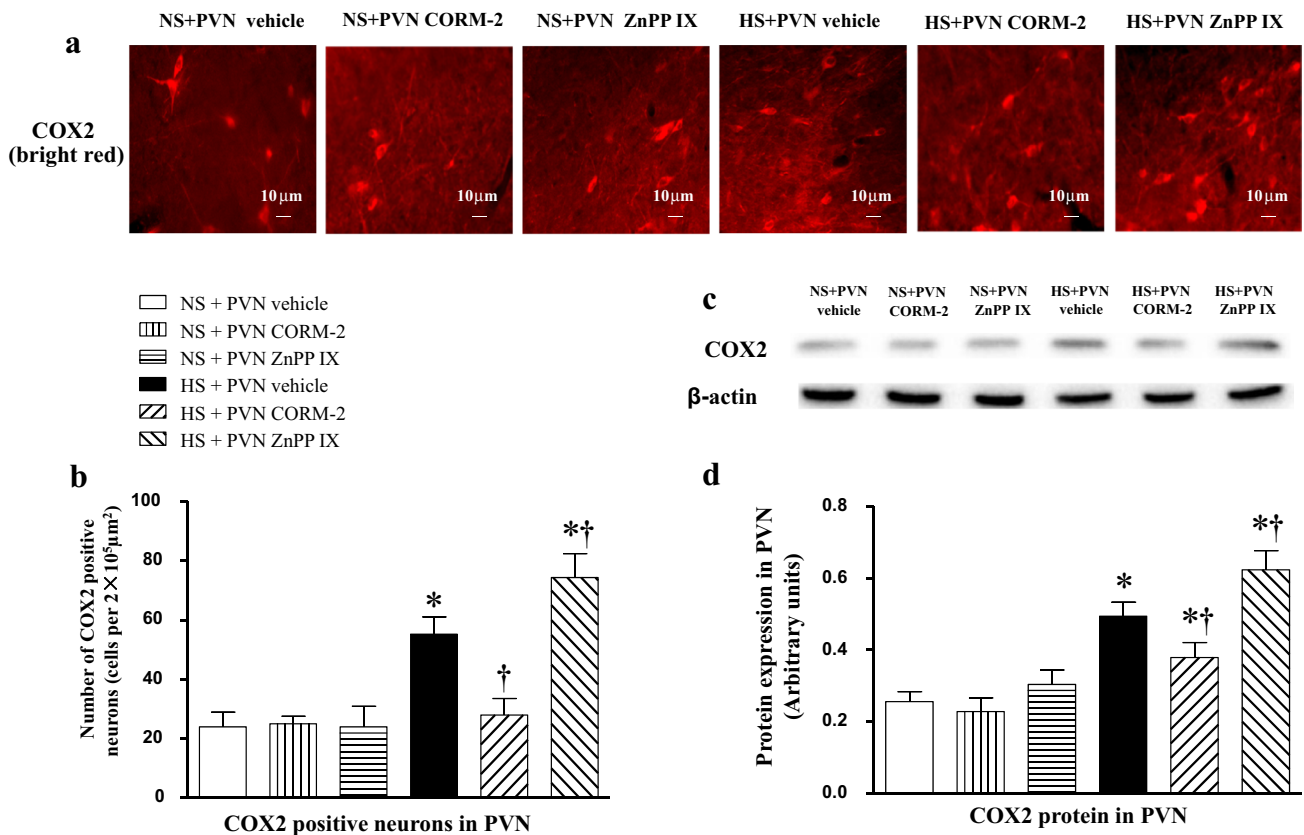


**Fig. 4** Effects of PVN infusion of CORM-2, ZnPP IX, or vehicle on the expressions of COX2 in PVN. The expressions of PVN COX2 in high-salt diet rats were higher than in normal-salt diet rats, but decreased significantly in the HS+CORM-2 group and increased significantly in the HS+ZnPP IX group ( $p < 0.05$ , each group  $n = 7$ ). (a) Representative immunofluorescence staining of COX2. (b) Den-

sitometric analysis of immunofluorescent intensity of COX2 in the PVN. (c) Representative immunoblot of COX2 in the PVN. (d) Densitometric analysis of protein expression of COX2 in the PVN. Values are expressed as mean  $\pm$  SEM. \* $p < 0.05$  versus control (NS groups); † $p < 0.05$  HS+PVN CORM-2 or ZnPP IX versus HS+PVN vehicle

## Results

### Mean Arterial Pressure (MAP)

MAP was elevated for 10 weeks, which was measured weekly by the tail-cuff method and the last time by the femoral artery cannula. Evaluation showed that MAP increased with time of high-salt diet in HS groups. It was changed at the 3rd week after high-salt diet. And MAP increased significantly at the 4th week in HS groups compared to the NS groups ( $p < 0.05$ ). Treatment with PVN infusion of CORM-2 reduced MAP significantly in high salt-induced hypertensive rats, compared to the high-salt diet rats treated by vehicle ( $p < 0.05$ ). But treatment with PVN infusion of ZnPP IX increased MAP compared with the HS + PVN vehicle group ( $p < 0.05$ ) (Fig. 1).

### Renal Sympathetic Nerve Activity (RSNA)

High-salt diet increased the ratio of basal RSNA to max RSNA ( $p < 0.05$ ) (Fig. 2), but decreased max RSNA ( $p < 0.05$ ) (Table 1). Treatment with PVN infusion of CORM-2 weakened RSNA significantly in high salt-induced hypertensive rats, compared to the high-salt diet rats treated by vehicle ( $p < 0.05$ ). But treatment with PVN infusion of ZnPP IX increased RSNA compared to the HS + PVN vehicle group ( $p < 0.05$ ) (Fig. 2).

### The Levels of Plasma NE

Plasma NE was measured by ELISA. The levels of plasma NE increased significantly in the groups of high-salt diet, compared to the groups of normal-salt diet ( $p < 0.05$ ). The levels of plasma NE was decreased significantly in the

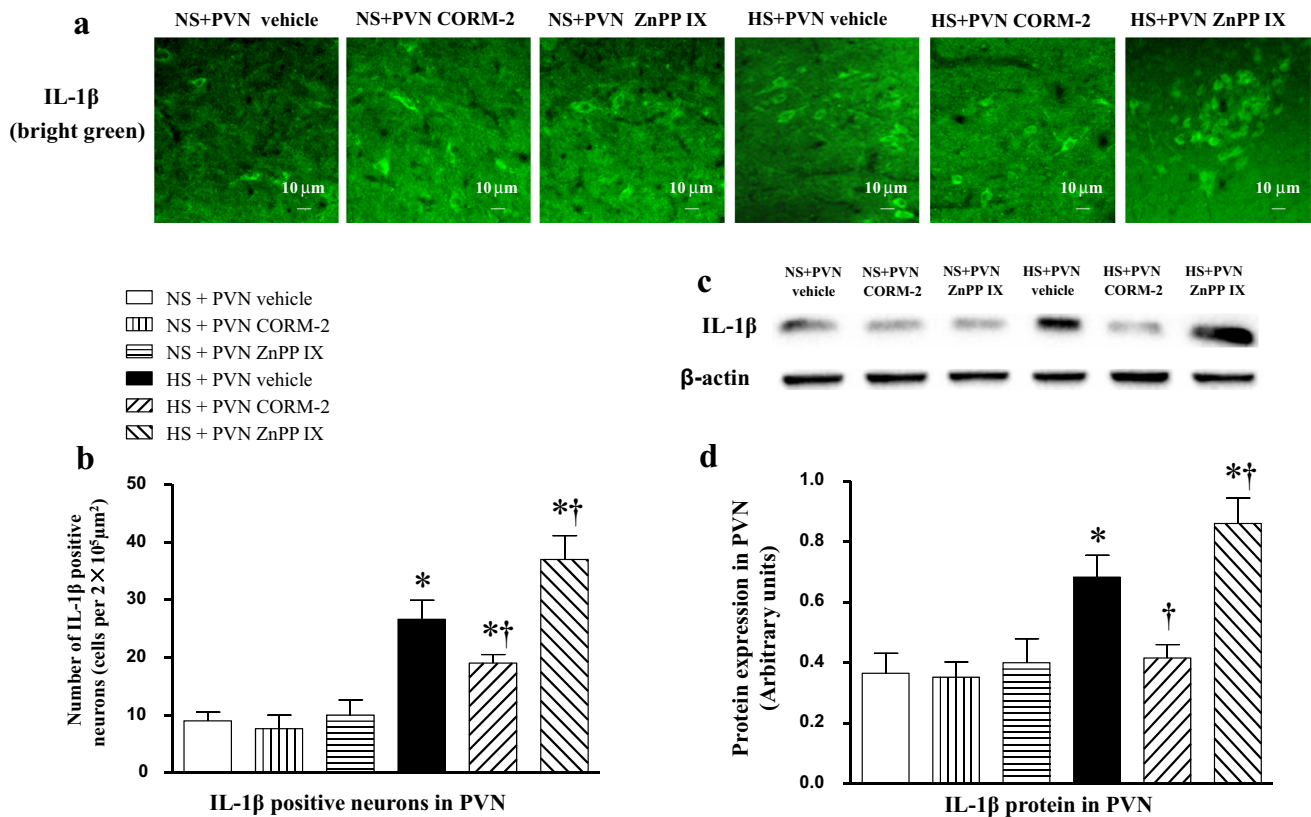


**Fig. 5** Effects of PVN infusion of CORM-2, ZnPP IX, or vehicle on the expressions of IL-1 $\beta$  in PVN. The expressions of PVN IL-1 $\beta$  in high-salt diet rats were higher than in normal-salt diet rats, but decreased significantly in the HS+CORM-2 group and increased significantly in the HS+ZnPP IX group ( $p < 0.05$ , each group  $n = 7$ ). **a** Representative immunofluorescence staining of IL-1 $\beta$ . **b** Densi-

tometric analysis of immunofluorescent intensity of IL-1 $\beta$  in the PVN. **c** Representative immunoblot of IL-1 $\beta$  in the PVN. **d** Densitometric analysis of protein expression of IL-1 $\beta$  in the PVN. Values are expressed as mean  $\pm$  SEM. \* $p < 0.05$  versus control (NS groups); † $p < 0.05$  HS + PVN CORM-2 or ZnPP IX versus HS + PVN vehicle

HS + PVN CORM-2 group, but increased significantly in the HS + PVN ZnPP IX group, compared to the HS + PVN vehicle group ( $p < 0.05$ ) (Fig. 2).

### HO-1 Expression in the PVN

Immunofluorescence staining and western blot were performed to study the expression of HO-1. HO-1 expression in PVN was decreased significantly in the HS groups, which was compared to the NS groups ( $p < 0.05$ ). Bilateral microinjection of CORM-2 into the PVN increased the HO-1 expression significantly in this region, while bilateral microinjection of ZnPP IX aggravated the decreased HO-1 expression, compared to the HS + PVN vehicle group ( $p < 0.05$ ) (Fig. 3).

### Cyclooxygenase-2 (COX-2) Expression in the PVN

From the results of immunofluorescence staining and western blot, COX-2 expression in PVN was increased

significantly in the HS groups, which is compared to the NS groups ( $p < 0.05$ ). Bilateral microinjection of CORM-2 into the PVN decreased the COX-2 expression significantly, while bilateral microinjection of ZnPP IX increased COX-2 expression, compared to the HS + PVN vehicle group ( $p < 0.05$ ) (Fig. 4).

### Pro-inflammatory Cytokines (PICs) Expression in the PVN

High-salt diet induced significant increase of IL-1 $\beta$ , IL-6 in the PVN ( $p < 0.05$ ). Bilateral microinjection of CORM-2 into the PVN reduced the expressions of IL-1 $\beta$  and IL-6 significantly induced by high-salt diet, while PVN infusion of ZnPP IX exacerbated the expressions of these cytokines in the PVN, compared to the HS + PVN vehicle group ( $p < 0.05$ ) (Figs. 5 and 6).

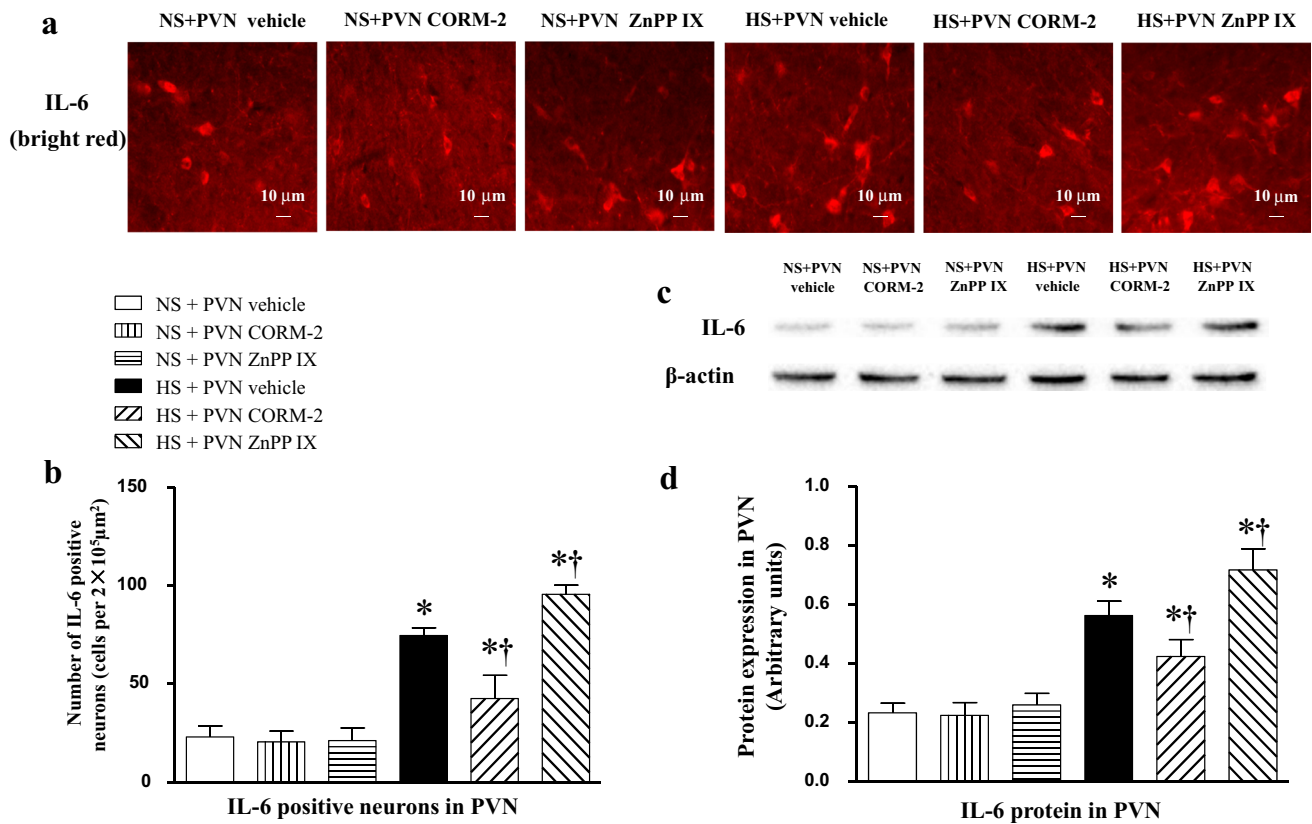


**Fig. 6** Effects of PVN infusion of CORM-2, ZnPP IX, or vehicle on the expressions of IL-6 in PVN. The expressions of PVN IL-6 in high-salt diet rats were higher than in normal-salt diet rats, but decreased significantly in the HS+CORM-2 group and increased significantly in the HS+ZnPP IX group ( $p < 0.05$ , each group  $n = 7$ ). **a** Representative immunofluorescence staining of IL-6. **b** Densito-

metric analysis of immunofluorescent intensity of IL-6 in the PVN. **c** Representative immunoblot of IL-6 in the PVN. **d** Densitometric analysis of protein expression of IL-6 in the PVN. Values are expressed as mean  $\pm$  SEM. \* $p < 0.05$  versus control (NS groups); † $p < 0.05$  HS + PVN CORM-2 or ZnPP IX versus HS + PVN vehicle

## Oxidative Stress Parameters in the PVN

The expressions of NOX2 and NOX4, the NAD(P)H oxidase subunits, in the PVN were increased significantly in high-salt diet groups compared to control groups ( $p < 0.05$ ) (Figs. 7 and 8). High-salt diet induced an increase of ROS level as determined by fluorescent-labeled dihydroethidium (DHE) staining ( $p < 0.05$ ) (Fig. 9). Bilateral microinjection of CORM-2 into the PVN decreased the expressions of NOX2, NOX4, and the level of ROS significantly, while PVN infusion of ZnPP IX promoted the expressions of these parameters, compared to the HS + PVN vehicle group ( $p < 0.05$ ) (Figs. 7, 8, and 9). The expression of Cu/Zn-SOD in the PVN decreased significantly in the HS groups, compared to the NS groups ( $p < 0.05$ ). Bilateral microinjection of CORM-2 into the PVN increased the expression of Cu/Zn-SOD significantly, while PVN infusion of ZnPP IX decreased the expression of Cu/Zn-SOD, compared to the HS + PVN vehicle group ( $p < 0.05$ ) (Fig. 9).

## Discussions

The novel finding in this study is that CO in the PVN attenuates hypertensive responses and RSNA by decreasing the expressions of PICs and the oxidative stress responses.

In this study, we demonstrated that high-salt diet increased the levels of MAP in Dahl Salt-Sensitive rats, and decreased the levels of HO-1 in the PVN of rats. Then we detected the sympathetic nerve activity by RSNA, which is expressed as a percentage of maximum (in response to SNP). It has been reported that salt diet would limit the SNP-induced endothelium-independent relaxations [35], and the trend of SNP-stimulated max RSNA was significantly decreased by high-salt diet in our study. So the levels of plasma NE were detected in order to corroborate sympathetic nerve activity. Our results showed that high-salt diet increased the levels of plasma NE. It suggested that salt increased sympathetic activity as measured by circulating

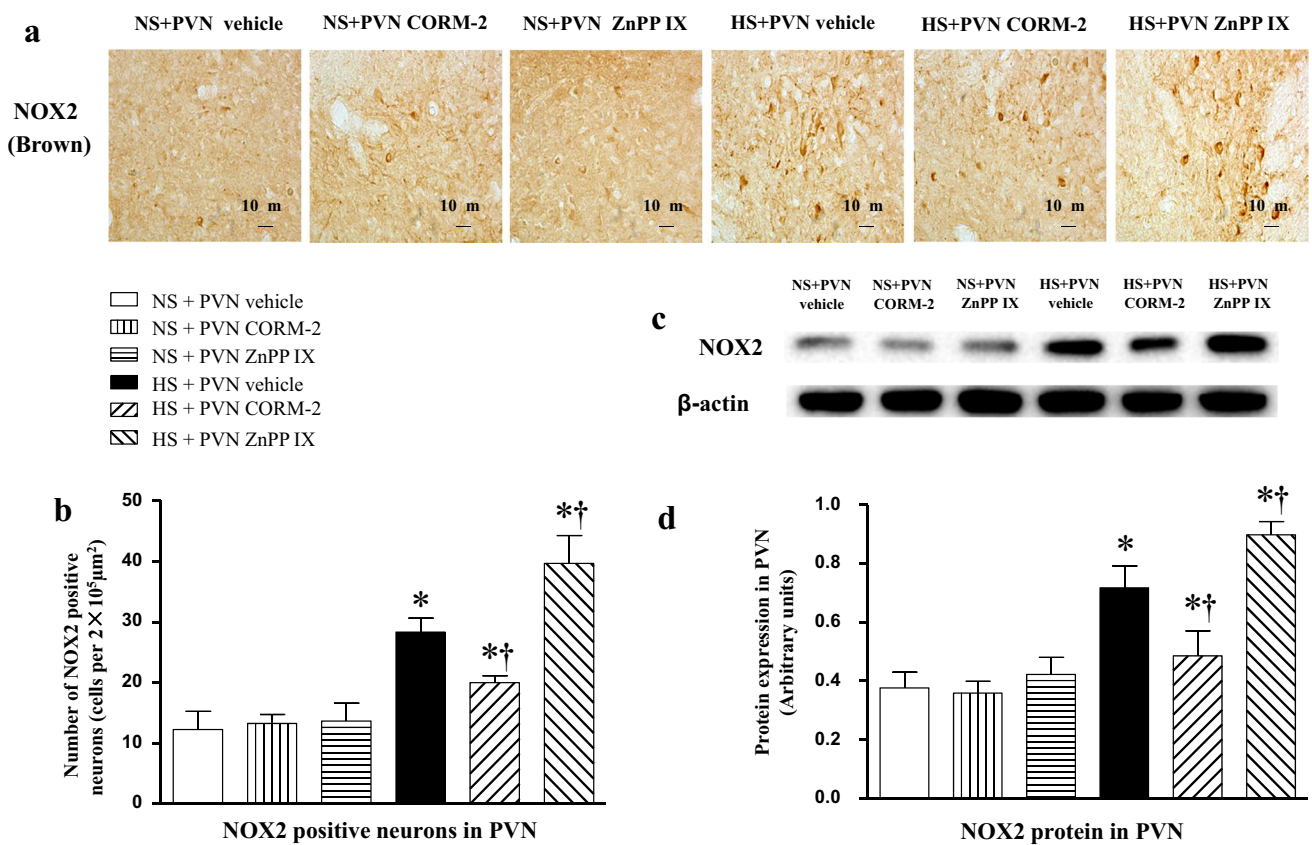


**Fig. 7** Effects of PVN infusion of CORM-2, ZnPP IX, or vehicle on the expressions of NOX2 in PVN. The expressions of PVN NOX2 in high-salt diet rats were higher than in normal-salt diet rats, but decreased significantly in the HS + CORM-2 group and increased significantly in the HS + ZnPP IX group ( $p < 0.05$ , each group  $n = 7$ ). **a** Representative immunohistochemical staining of NOX2 in the PVN.

**b** Densitometric analysis of immunohistochemical intensity of NOX2 in the PVN. **c** Representative immunoblot of NOX2 in the PVN. **d** Densitometric analysis of protein expression of NOX2 in the PVN. Values are expressed as mean  $\pm$  SEM. \* $p < 0.05$  versus control (NS groups); † $p < 0.05$  HS + PVN CORM-2 or ZnPP IX versus HS + PVN vehicle

norepinephrine, and increased the ratio of basal RSNA to max RSNA, in part by decreasing max RSNA. The results above suggested that the changes of PVN HO-1 and the peripheral sympathetic activity played an important role in high-salt diet induced hypertension. Results also showed that PVN infusion of CORM-2, an agent that releases CO from tricarbonyldichlororuthenium (II) dimer, made a hypotensive response, decreased RSNA and the levels of plasma NE, whereas microinjection into the PVN of ZnPP IX, the inhibitor of HO-1, was opposite to the effects of CORM-2. HO-1 catabolizes heme to bilirubin, CO, and free iron. And it has been reported that biliverdin was biologically an important antioxidant and potentially lowers BP [21, 27, 28]. So we focused on CORM-2 as the exogenous CO donor to confirm the effects of CO and ZnPP IX to assess the endogenous CO. These results implied that the exogenous or endogenous CO in the PVN reduced the sympathetic activity, resulting in a fall in blood pressure. Consistent with our results, several other recent studies showed that CO by the presence of HO

in nucleus tractus solitarius (NTS) produced hypotensive activity [36–39]. Furthermore, it has been shown that a significantly decreased BP was observed by intraperitoneal injection of HO inducer in spontaneously hypertensive rats (SHR), presumably via heme oxygenase-mediated formation of carbon monoxide [40]. This is an indication that CO can decrease blood pressure in hypertensive rats in both the central and peripheral nervous systems. Studies had documented that hypotensive response of CO in peripheral circulation was related to vasodepressive response [41, 42]. However, the hypotensive mechanism of CO in PVN is obscure. Our previous studies showed that increased PICs and ROS in the PVN or RVLM led to enhanced sympathetic activation and blood pressure in high salt- or Ang II-induced hypertension [43, 44], which was consistent with some other studies [45, 46]. Furthermore, CO has been identified to present antioxidation and anti-inflammatory properties [19–26]. We then investigated that whether the level of CO in the PVN

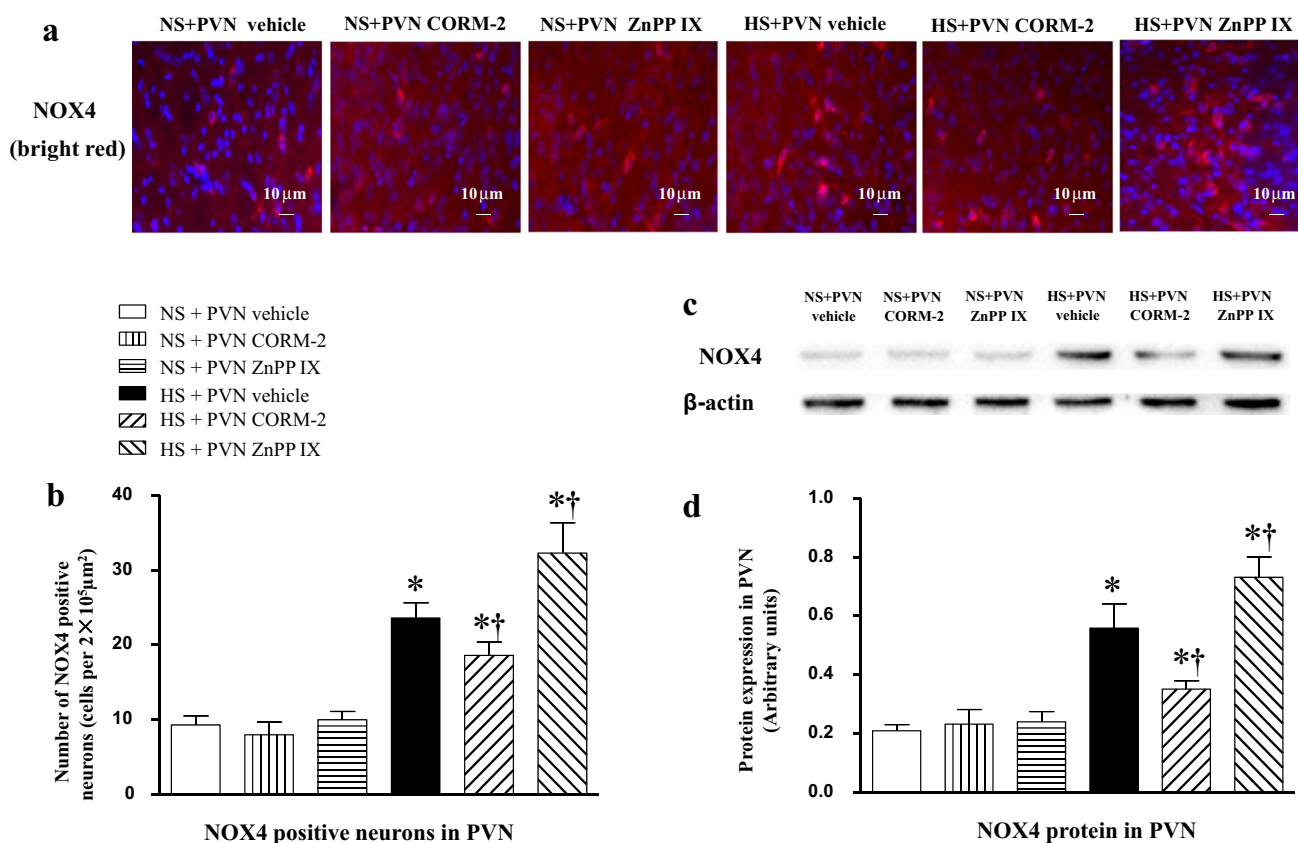


**Fig. 8** Effects of PVN infusion of CORM-2, ZnPP IX, or vehicle on the expressions of NOX4 in PVN. The expressions of PVN NOX4 in high-salt diet rats were higher than in normal-salt diet rats, but decreased significantly in the HS+CORM-2 group and increased significantly in the HS+ZnPP IX group ( $p < 0.05$ , each group  $n = 7$ ). **a** Representative immunofluorescence staining of NOX4. Neuronal

nuclei are shown in blue. **b** Densitometric analysis of immunofluorescent intensity of NOX4 in the PVN. **c** A representative immunoblot of NOX4 in the PVN. **d** Densitometric analysis of protein expression of NOX4 in the PVN. Values are expressed as mean  $\pm$  SEM. \* $p < 0.05$  versus control (NS groups); † $p < 0.05$  HS+PVN CORM-2 or ZnPP IX versus HS+PVN vehicle

affected the inflammatory cytokines and oxidative stress or not.

The results showed that the expressions of COX-2, IL-1 $\beta$ , and IL-6 increased significantly in the PVN of high salt diet-included hypertension in rats. It was further indicated that PICs in the PVN were closely related to hypertension induced by high-salt diet. Furthermore, our previous study showed that PVN microinjection of gevokizumab, an IL-1 $\beta$  inhibitor, attenuated hypertensive responses by downregulating the pro-inflammatory cytokines [47]. Cyclooxygenase-2 (COX-2) is an enzyme, which is responsible for the formation of prostanoids. Ho et al. [48] documented that the peripheral LPS-induced increases in IL-1 $\beta$  and IL-6 production in the hippocampus were appreciably blunted by infusion into the lateral ventricle of NS398, a COX-2 inhibitor. Another study showed that pretreatment with subfornical organ (SFO) microinjection of COX-2 inhibitor NS398 attenuated the expression of IL-1 $\beta$  in SFO and downstream in PVN and the IL-1 $\beta$ -induced pressor responses [49]. These findings and

our results suggested that high salt diet-induced hypertension was closely related to the increased PICs mediated by COX-2 in the PVN. Furthermore, our results also showed that CORM-2 microinjecting into PVN could increase the levels of HO-1 and downregulate the levels of COX-2, IL-1 $\beta$ , and IL-6 in the PVN of the high salt diet-induced hypertension in rats. And microinjection into the PVN of ZnPP IX could reverse these parameters. It suggests that exogenous and endogenous CO in the PVN may produce hypotension by reducing the expression of PVN COX-2, leading to the decrease of IL-1 $\beta$  and IL-6.

Our previous studies documented that oxidative stress in the PVN had been emerged as a critical role in regulating sympathoexcitation of salt-sensitive hypertension [50]. NAD(P)H oxidase (NOX) transfers electrons from Nicotinamide adenine dinucleotide phosphate, which is abbreviated as NAD(P)H, to molecular oxygen to generate ROS such as superoxide. It has been shown that the level of ROS was augmented following increased NOX in SHR, high salt-induced hypertension and angiotensin

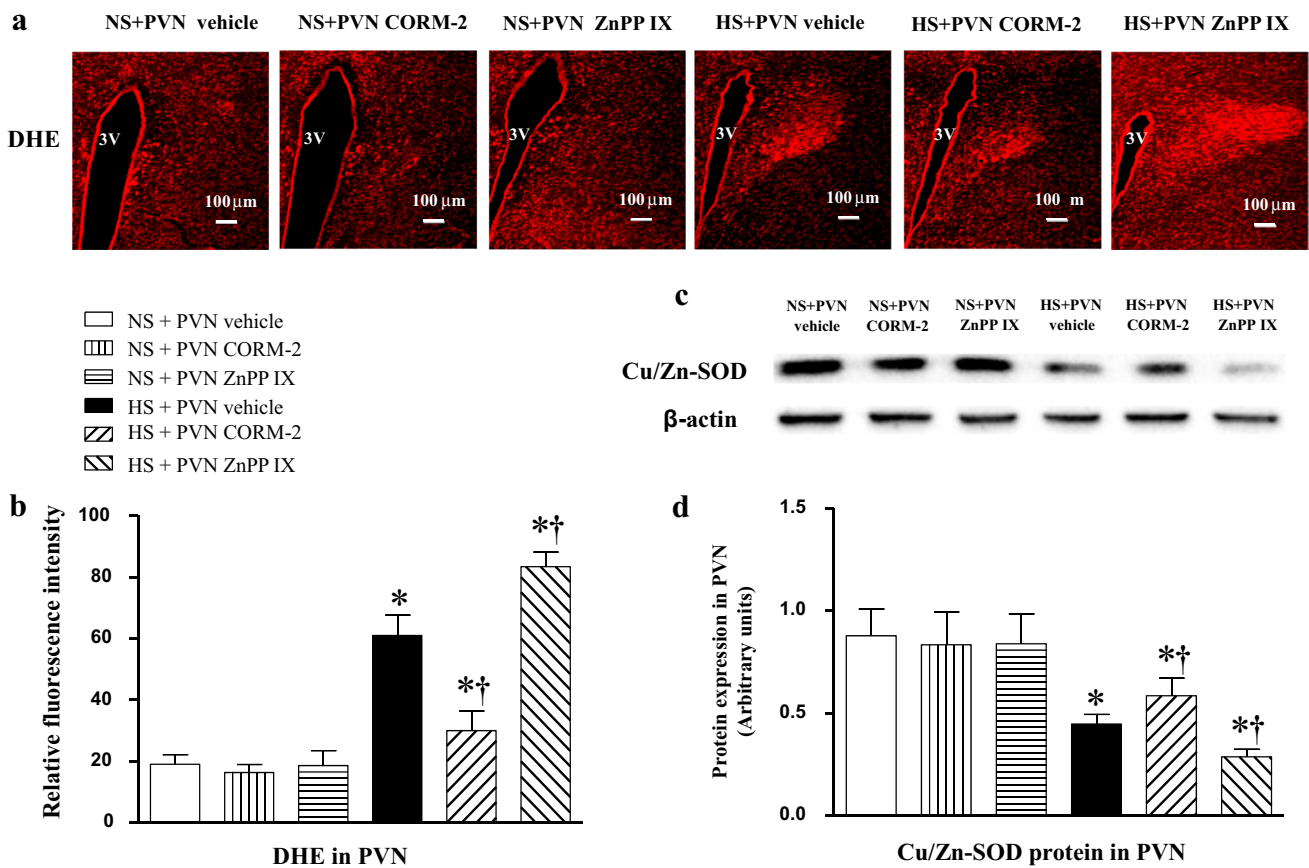


**Fig. 9** Effects of PVN infusion of CORM-2, ZnPP IX, or vehicle on the levels of the superoxide and the expressions of Cu/Zn-SOD protein in the PVN. ROS activity was measured by fluorescent-labeled dihydroethidium (DHE) staining and Cu/Zn-SOD proteins were measured by western blot. The levels of ROS in high-salt diet rats were higher than in normal-salt diet rats, but decreased significantly in the HS + CORM-2 group and increased significantly in the HS + ZnPP IX group ( $p < 0.05$ , each group  $n = 7$ ). The expressions of Cu/Zn-SOD in high-salt diet rats were lower than in normal-salt

diet rats, but increased significantly in the HS + CORM-2 group and decreased significantly in the HS + ZnPP IX group ( $p < 0.05$ , each group  $n = 7$ ). **a** Representative immunofluorescence image of DHE. **b** Densitometric analysis of immunofluorescent intensity of DHE in the PVN. **c** Representative immunoblot of Cu/Zn-SOD. **d** Densitometric analysis of protein expression of Cu/Zn-SOD in the PVN. Values are expressed as mean  $\pm$  SEM. \* $p < 0.05$  versus control (NS groups); † $p < 0.05$  HS + PVN CORM-2 or ZnPP IX versus HS + PVN vehicle. 3V third ventricle

II-induced hypertension [33, 51, 52]. In this study, we found that high-salt diet increased the expressions of NOX2 and NOX4 in the PVN, as compared with normal-salt diet. But the expression of PVN Cu/Zn superoxide dismutase (Cu/Zn-SOD) was decreased by high salt diet. And the level of ROS in the PVN was significantly increased in HS groups. NOX transfers electrons to molecular oxygen to generate ROS, an important mediator of oxidative stress [16]. Cu/Zn-SOD, a primary cytoplasmic antioxidant enzyme, scavenges oxygen radicals. The changes of PVN NOX2, NOX4, Cu/Zn-SOD, and ROS in this study provided further evidence that sympathoexcitation promoted salt-sensitive hypertension via oxidative stress in the PVN. Additionally, data from this study showed that bilateral microinjection of CORM-2 into PVN ameliorated the increased expressions of NOX2, NOX4, and ROS and the decreased expression of Cu/Zn-SOD in the PVN in high-salt diet groups. But ZnPP IX

microinjecting into PVN increased expressions of NOX2, NOX4, and ROS and the decreased expression of Cu/Zn-SOD in the PVN in high-salt diet groups. It indicated that exogenous and endogenous CO in the PVN reduced the peripheral sympathetic activation and blood pressure via antioxidant function.

In conclusion, the major finding of this study is that exogenous or endogenous CO within the PVN might have potential antihypertensive treatment by downregulating COX2 and PICs in the PVN and by reducing PVN oxidative stress-mediated sympathetic activity in high salt-induced hypertension. Our findings provide the rationale for the prevention and treatment of high salt diet-induced hypertension by increasing the level of CO in the PVN. However, further research is needed to clarify the pathway for the changes of PICs and oxidative stress response influenced by CO in the PVN.

## Conclusions

These findings suggest that exogenous or endogenous CO in the PVN may produce hypotensive response, which are partly due to decreased PICs and oxidative stress within the PVN in high salt-induced hypertension.

**Acknowledgements** We thank Xin-ai Song for technical assistance. This work was supported by National Natural Science Foundation of China (Grant Numbers 81770426, 91439120, 81600330, 81600333), China Postdoctoral Science Foundation (Nos. 2016M590957, 2016M602835), Shaanxi Postdoctoral Science Foundation (Nos. 2016BSHEDZZ89, 2016BSHEDZZ91), and the Foundation of Jiamusi University (Grant Number Sq2014-001).

**Author Contributions** YK, XY, and DZ designed the study. DZ, YL, JQ, HG, KL, YC, XS, GX, and LF performed all experiments. DZ and YL also performed data analysis and drafted the manuscript. YK, WC, JQ, and KK critically revised the manuscript. All authors reviewed the final manuscript.

## Compliance with Ethical Standards

**Conflict of interest** The authors declare that there is no conflict of interests regarding the publication of this paper.

## References

- Frohlich, E. D., & Varagic, J. (2005). Sodium directly impairs target organ function in hypertension. *Curr Opin Cardiol*, *20*, 424–429.
- Ha, S. K. (2014). Dietary salt intake and hypertension. *Electrolyte Blood Press*, *12*, 7–18.
- Yu, X. J., Suo, Y. P., Qi, J., Yang, Q., Li, H. H., Zhang, D. M., et al. (2013). Interaction between AT1 receptor and NF-kappaB in hypothalamic paraventricular nucleus contributes to oxidative stress and sympathoexcitation by modulating neurotransmitters in heart failure. *Cardiovasc Toxicol*, *13*, 381–390.
- Su, Q., Qin, D. N., Wang, F. X., Ren, J., Li, H. B., Zhang, M., et al. (2014). Inhibition of reactive oxygen species in hypothalamic paraventricular nucleus attenuates the renin-angiotensin system and proinflammatory cytokines in hypertension. *Toxicol Appl Pharmacol*, *276*, 115–120.
- Cardinale, J. P., Sriramula, S., Mariappan, N., Agarwal, D., & Francis, J. (2012). Angiotensin II-induced hypertension is modulated by nuclear factor-kappaB in the paraventricular nucleus. *Hypertension*, *59*, 113–121.
- Kang, Y. M., Zhang, D. M., Yu, X. J., Yang, Q., Qi, J., Su, Q., et al. (2014). Chronic infusion of enalaprilat into hypothalamic paraventricular nucleus attenuates angiotensin II-induced hypertension and cardiac hypertrophy by restoring neurotransmitters and cytokines. *Toxicol Appl Pharmacol*, *274*, 436–444.
- Swanson, L. W., & Sawchenko, P. E. (1980). Paraventricular nucleus: a site for the integration of neuroendocrine and autonomic mechanisms. *Neuroendocrinology*, *31*, 410–417.
- Levitt, D. G., & Levitt, M. D. (2015). Carbon monoxide: a critical quantitative analysis and review of the extent and limitations of its second messenger function. *Clin Pharmacol*, *7*, 37–56.
- Maines, M. D. (1997). The heme oxygenase system: a regulator of second messenger gases. *Annu Rev Pharmacol Toxicol*, *37*, 517–554.
- Ewing, J. F., & Maines, M. D. (1992). In situ hybridization and immunohistochemical localization of heme oxygenase-2 mRNA and protein in normal rat brain: differential distribution of isozyme 1 and 2. *Mol Cell Neurosci*, *3*, 559–570.
- Vincent, S. R., Das, S., & Maines, M. D. (1994). Brain heme oxygenase isoenzymes and nitric oxide synthase are co-localized in select neurons. *Neuroscience*, *63*, 223–231.
- Leffler, C. W., Parfenova, H., & Jaggar, J. H. (2011). Carbon monoxide as an endogenous vascular modulator. *Am J Physiol Heart Circ Physiol*, *301*, H1–H11.
- Granger, J. P. (2006). An emerging role for inflammatory cytokines in hypertension. *Am J Physiol Heart Circ Physiol*, *290*, H923–H924.
- Guzik, T. J., & Touyz, R. M. (2017). Oxidative stress, inflammation, and vascular aging in hypertension. *Hypertension*, *70*, 660–667.
- Naregal, G. V., Devaranavadi, B. B., Patil, S. G., & Aski, B. S. (2017). Elevation of oxidative stress and decline in endogenous antioxidant defense in elderly individuals with hypertension. *J Clin Diagn Res*, *11*, BC09–BC12.
- Harayama, S., Kok, M., & Neidle, E. L. (1992). Functional and evolutionary relationships among diverse oxygenases. *Annu Rev Microbiol*, *46*, 565–601.
- Bai, J., Yu, X. J., Liu, K. L., Wang, F. F., Jing, G. X., Li, H. B., et al. (2017). Central administration of tert-butylhydroquinone attenuates hypertension via regulating Nrf2 signaling in the hypothalamic paraventricular nucleus of hypertensive rats. *Toxicol Appl Pharmacol*, *333*, 100–109.
- Liang, Y. F., Zhang, D. D., Yu, X. J., Gao, H. L., Liu, K. L., Qi, J., et al. (2017). Hydrogen sulfide in paraventricular nucleus attenuates blood pressure by regulating oxidative stress and inflammatory cytokines in high salt-induced hypertension. *Toxicol Lett*, *270*, 62–71.
- Gorojod, R. M., Alaimo, A., Porte Alcon, S., Martinez, J. H., Cortina, M. E., Vazquez, E. S., et al. (2018). Heme oxygenase-1 protects astroglia against manganese-induced oxidative injury by regulating mitochondrial quality control. *Toxicol Lett*, *295*, 357–368.
- Berne, J. P., Lauzier, B., Rochette, L., & Vergely, C. (2012). Carbon monoxide protects against ischemia-reperfusion injury in vitro via antioxidant properties. *Cell Physiol Biochem*, *29*, 475–484.
- Parfenova, H., Leffler, C. W., Basuroy, S., Liu, J., & Fedinec, A. L. (2012). Antioxidant roles of heme oxygenase, carbon monoxide, and bilirubin in cerebral circulation during seizures. *J Cereb Blood Flow Metab*, *32*, 1024–1034.
- Lian, S., Xia, Y., Ung, T. T., Khoi, P. N., Yoon, H. J., Kim, N. H., et al. (2016). Carbon monoxide releasing molecule-2 ameliorates IL-1beta-induced IL-8 in human gastric cancer cells. *Toxicology*, *361–362*, 24–38.
- Bauer, B., Goderz, A. L., Braumuller, H., Neudorfl, J. M., Rocken, M., Wieder, T., et al. (2017). Methyl fumarate-derived iron carbonyl complexes (FumET-CORMs) as powerful anti-inflammatory agents. *ChemMedChem*, *12*, 1927–1930.
- Choi, S., Kim, J., Kim, J. H., Lee, D. K., Park, W., Park, M., et al. (2017). Carbon monoxide prevents TNF-alpha-induced eNOS downregulation by inhibiting NF-kappaB-responsive miR-155-5p biogenesis. *Exp Mol Med*, *49*, e403.
- Lin, C. C., Yang, C. C., Hsiao, L. D., Chen, S. Y., & Yang, C. M. (2017). Heme oxygenase-1 induction by carbon monoxide releasing molecule-3 suppresses interleukin-1 beta-mediated neuroinflammation. *Front Mol Neurosci*, *10*, 387.
- Sun, Q., Wu, Y., Zhao, F., & Wang, J. (2017). Maresin 1 ameliorates lung ischemia/reperfusion injury by suppressing oxidative stress via activation of the Nrf-2-mediated HO-1 signaling pathway. *Oxid Med Cell Longev*, *2017*, 9634803.

27. Stocker, R., McDonagh, A. F., Glazer, A. N., & Ames, B. N. (1990). Antioxidant activities of bile pigments: biliverdin and bilirubin. *Methods Enzymol*, *186*, 301–309.
28. Chen, W., Maghzal, G. J., Ayer, A., Suarna, C., Dunn, L. L., & Stocker, R. (2018). Absence of the biliverdin reductase-a gene is associated with increased endogenous oxidative stress. *Free Radic Biol Med*, *115*, 156–165.
29. Nassar, N. N., Li, G., Strat, A. L., & Abdel-Rahman, A. A. (2011). Enhanced hemeoxygenase activity in the rostral ventrolateral medulla mediates exaggerated hemin-evoked hypotension in the spontaneously hypertensive rat. *J Pharmacol Exp Ther*, *339*, 267–274.
30. Fouda, M. A., El-Gowell, H. M., El-Gowilly, S. M., Rashed, L., & El-Mas, M. M. (2014). Impairment of nitric oxide synthase but not heme oxygenase accounts for baroreflex dysfunction caused by chronic nicotine in female rats. *PLoS ONE*, *9*, e98681.
31. Qi, J., Zhang, D. M., Suo, Y. P., Song, X. A., Yu, X. J., Elks, C., et al. (2013). Renin-angiotensin system modulates neurotransmitters in the paraventricular nucleus and contributes to angiotensin II-induced hypertensive response. *Cardiovasc Toxicol*, *13*, 48–54.
32. Li, H. B., Qin, D. N., Ma, L., Miao, Y. W., Zhang, D. M., Lu, Y., et al. (2014). Chronic infusion of lisinopril into hypothalamic paraventricular nucleus modulates cytokines and attenuates oxidative stress in rostral ventrolateral medulla in hypertension. *Toxicol Appl Pharmacol*, *279*, 141–149.
33. Zhang, M., Qin, D. N., Suo, Y. P., Su, Q., Li, H. B., Miao, Y. W., et al. (2015). Endogenous hydrogen peroxide in the hypothalamic paraventricular nucleus regulates neurohormonal excitation in high salt-induced hypertension. *Toxicol Lett*, *235*, 206–215.
34. Kang, Y. M., Gao, F., Li, H. H., Cardinale, J. P., Elks, C., Zang, W. J., et al. (2011). NF-kappaB in the paraventricular nucleus modulates neurotransmitters and contributes to sympathoexcitation in heart failure. *Basic Res Cardiol*, *106*, 1087–1097.
35. Kagota, S., Tamashiro, A., Yamaguchi, Y., Nakamura, K., & Kunitomo, M. (2002). High salt intake impairs vascular nitric oxide/cyclic guanosine monophosphate system in spontaneously hypertensive rats. *J Pharmacol Exp Ther*, *302*, 344–351.
36. Johnson, R. A., Colombari, E., Colombari, D. S., Lavesa, M., Talman, W. T., & Nasjletti, A. (1997). Role of endogenous carbon monoxide in central regulation of arterial pressure. *Hypertension*, *30*, 962–967.
37. Lo, W. C., Jan, C. R., Chiang, H. T., & Tseng, C. J. (2000). Modulatory effects of carbon monoxide on baroreflex activation in nucleus tractus solitarii of rats. *Hypertension*, *35*, 1253–1257.
38. Lo, W. C., Chan, J. Y., Tung, C. S., & Tseng, C. J. (2002). Carbon monoxide and metabotropic glutamate receptors in rat nucleus tractus solitarii: participation in cardiovascular effect. *Eur J Pharmacol*, *454*, 39–45.
39. Lin, C. H., Lo, W. C., Hsiao, M., & Tseng, C. J. (2003). Interaction of carbon monoxide and adenosine in the nucleus tractus solitarii of rats. *Hypertension*, *42*, 380–385.
40. Johnson, R. A., Lavesa, M., DeSeyn, K., Scholer, M. J., & Nasjletti, A. (1996). Heme oxygenase substrates acutely lower blood pressure in hypertensive rats. *Am J Physiol*, *271*, H1132–H1138.
41. Johnson, R. A., Lavesa, M., Askari, B., Abraham, N. G., & Nasjletti, A. (1995). A heme oxygenase product, presumably carbon monoxide, mediates a vasodepressor function in rats. *Hypertension*, *25*, 166–169.
42. Bolognesi, M., Sacerdoti, D., Piva, A., Di Pascoli, M., Zampieri, F., Quarta, S., et al. (2007). Carbon monoxide-mediated activation of large-conductance calcium-activated potassium channels contributes to mesenteric vasodilatation in cirrhotic rats. *J Pharmacol Exp Ther*, *321*, 187–194.
43. Wang, M. L., Yu, X. J., Li, X. G., Pang, D. Z., Su, Q., Saahene, R. O., et al. (2018). Blockade of TLR4 within the paraventricular nucleus attenuates blood pressure by regulating ROS and inflammatory cytokines in prehypertensive rats. *Am J Hypertens*, *31*, 1013–1023.
44. Kang, Y. M., Yang, Q., Yu, X. J., Qi, J., Zhang, Y., Li, H. B., et al. (2014). Hypothalamic paraventricular nucleus activation contributes to neurohumoral excitation in rats with heart failure. *Regen Med Res*, *2*, 2.
45. Shi, P., Diez-Freire, C., Jun, J. Y., Qi, Y., Katovich, M. J., Li, Q., et al. (2010). Brain microglial cytokines in neurogenic hypertension. *Hypertension*, *56*, 297–303.
46. Sriramula, S., Cardinale, J. P., & Francis, J. (2013). Inhibition of TNF in the brain reverses alterations in RAS components and attenuates angiotensin II-induced hypertension. *PLoS ONE*, *8*, e63847.
47. Qi, J., Zhao, X. F., Yu, X. J., Yi, Q. Y., Shi, X. L., Tan, H., et al. (2016). Targeting interleukin-1 beta to suppress sympathoexcitation in hypothalamic paraventricular nucleus in Dahl salt-sensitive hypertensive rats. *Cardiovasc Toxicol*, *16*, 298–306.
48. Ho, Y. H., Lin, Y. T., Wu, C. W., Chao, Y. M., Chang, A. Y., & Chan, J. Y. (2015). Peripheral inflammation increases seizure susceptibility via the induction of neuroinflammation and oxidative stress in the hippocampus. *J Biomed Sci*, *22*, 46.
49. Wei, S. G., Yu, Y., & Felder, R. B. (2018). Blood-borne interleukin-1beta acts on the subfornical organ to upregulate the sympathoexcitatory milieu of the hypothalamic paraventricular nucleus. *Am J Physiol Regul Integr Comp Physiol*, *314*, R447–R458.
50. Qi, J., Yu, X. J., Shi, X. L., Gao, H. L., Yi, Q. Y., Tan, H., et al. (2016). NF-kappaB blockade in hypothalamic paraventricular nucleus inhibits high-salt-induced hypertension through NLRP3 and Caspase-1. *Cardiovasc Toxicol*, *16*, 345–354.
51. Kang, Y. M., He, R. L., Yang, L. M., Qin, D. N., Guggilam, A., Elks, C., et al. (2009). Brain tumour necrosis factor-alpha modulates neurotransmitters in hypothalamic paraventricular nucleus in heart failure. *Cardiovasc Res*, *83*, 737–746.
52. Li, H. B., Qin, D. N., Cheng, K., Su, Q., Miao, Y. W., Guo, J., et al. (2015). Central blockade of salusin beta attenuates hypertension and hypothalamic inflammation in spontaneously hypertensive rats. *Sci Rep*, *5*, 11162.

**Publisher's Note** Springer Nature remains neutral with regard to jurisdictional claims in published maps and institutional affiliations.

## Affiliations

Dong-Dong Zhang<sup>1,3</sup> · Yan-Feng Liang<sup>1,4</sup> · Jie Qi<sup>1</sup> · Kai B. Kang<sup>5</sup> · Xiao-Jing Yu<sup>1</sup> · Hong-Li Gao<sup>1</sup> · Kai-Li Liu<sup>1</sup> · Yan-Mei Chen<sup>1</sup> · Xiao-Lian Shi<sup>6</sup> · Guo-Rui Xin<sup>1</sup> · Li-Yan Fu<sup>1</sup> · Yu-Ming Kang<sup>1</sup> · Wei Cui<sup>2</sup>

<sup>1</sup> Department of Physiology and Pathophysiology, Xi'an Jiaotong University School of Basic Medical Sciences, Key Laboratory of Environment and Genes Related to Diseases of Ministry of Education, Xi'an Jiaotong University, Xi'an 710061, China

<sup>2</sup> Department of Endocrinology and Metabolism, The First Affiliated Hospital of Xi'an Jiaotong University, Xi'an Jiaotong University Health Science Center, Xi'an 710061, China

<sup>3</sup> Department of Anatomy, School of Basic Medical Sciences, Jiamusi University, Jiamusi 154007, China

<sup>4</sup> Department of Pathophysiology, School of Basic Medical Sciences, Jiamusi University, Jiamusi 154007, China

<sup>5</sup> Department of Ophthalmology and Visual Sciences, University of Illinois at Chicago, Chicago, IL, USA

<sup>6</sup> Department of Pharmacology, School of Basic Medical Sciences, Xi'an Jiaotong University Health Science Center, Xi'an 710061, China